Field Emission Studies of Placed Emitters in the Mushroom Cavity

Janice Wynn and Dan Kapner
Cornell University

February 13, 1998
SRF9880511-03

Abstract

The superconducting niobium "mushroom" cavity has been used to study field emission and emitter processing of intentionally placed emitters. Nickel, molybdenum disulfide, and glassy carbon splinters ranging in size from 0.5 - 5 μm have been placed on the high E-field dimple of the mushroom plate. Foreign particles on the dimple were analyzed and photographed with a scanning electron microscope before and after RF testing. There was no change in any of the placed particles, though changes occurred in other particles present: one silicon exploded, several melted, and portions of a carbon particle disappeared.

1 Introduction

Field emission occurs in superconducting RF cavities when foreign particles are present. Cavities are used in accelerator physics applications such as the Cornell Electron Storage Ring (CESR). Field emission causes the quality factor (Q) of a cavity to fall and can limit the peak attainable fields. Thus it is desirable to eliminate field emitters from a cavity. Great steps have been made in reducing the number of emitters and in processing those that remain. Field emission and processing are not completely understood, though a solid theory base has been established. The goal of this study is to deepen our understanding of field emission and processing events by correlating the before, during, and after stages of emission. We hope to determine what properties of a particle (e.g. size, geometry, and elemental composition) make it a likely field emitter. We would also like to correlate these properties to the observable results of field emission and processing events. Examples of observable results are melting, altered appearance or disappearance of the particle, starburst patterns, craters, ripples, and the E-field at which the emission began. These conclusions will bear evidence to existing theories and provide a basis for new hypotheses.

This paper will begin with a summary of field emission theory, followed by an overview of our equipment, in particular the cavity design. Then our step by

step procedure for preparing and testing a mushroom plate will be described, as well as an overview of the intentions and outcomes of each cavity test. Finally, we will conclude with a description and discussion of our results, at the heart of which is a violently exploded silicon particle.

2 Fundamentals of Field Emission Theory

Field emission occurs when electrons tunnel out of the potential barrier at the surface of a metal. The electrostatic barrier in a field free region becomes nearly triangular due to the presence of an electric field component normal to the surface and to the image charge effect of the metal. If the field is large enough, the electron will be able to tunnel across this triangular potential. The Fowler-Nordheim (FN) relation [1] gives the expected tunneling current density as a function of the electric field and the work function of the metal. However, the current densities measured from field emission studies with DC electrodes and superconducting RF cavities are much greater than the standard FN current density. It has been found that field emission corresponds to the location of foreign particles on the metal surface. Studies have also shown that the current density as a function of field behaves according to the FN equation if E is enhanced by a factor β_{FN}, typically β_{FN} is several 100. Current theory holds that the high β_{FN} value is at least partially due to geometrical field enhancement by the foreign particle.

If the current density from the tip of a metallic emitter exceeds $\sim 10^{11}$ to 10^{12} A/m^2 the tip will melt. Often an emitter will explode or "process". During field emission, the emitted electrons ionize gas atoms near the emitter. The source of this gas is mostly vapor from the heated particle and the niobium. If the density of this ionic plasma becomes great enough a spark can occur. This spark is accompanied by the explosion of the particle and produces a starburst pattern several 100 μm across (see Figure 1). Starbursts are fluorine depleted areas and are only visible in the SEM. Often one or more craters of molten Nb are found at the center of the starburst. If the foreign particle is missing, there is usually still a thin layer of it on the surface near the central crater.

There are still many unknowns regarding field emission and processing. Emitters often do not have enough jagged edges to enhance the field by the observed β_{FN}. Nor is the timing of the plasma explosion creating the starburst fully understood. It was thought that the starburst occured simultaneously with the explosion of the particle, but sites have been found where the emitter was still active and/or melted, and yet a starburst was present [2]. This indicates that the starburst can be created before processing of the emitter. Finally, it is not known whether an emitter must completely melt before processing can occur. For further details beyond the scope of this paper, consult reference [1].

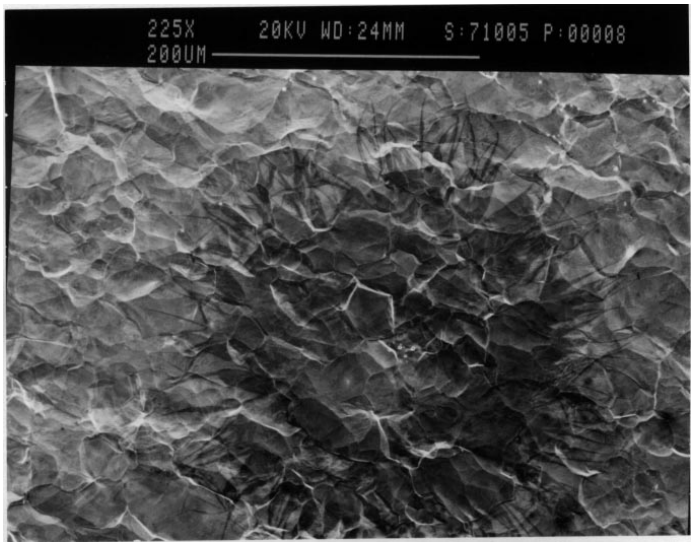

Figure 1: A starburst found after one of our tests. The darker region forming the starburst is an area depleted in flourine. Note the craters near the center of the starburst.

3 Equipment

The mushroom test cavity is ideal for our studies because of its removable plate that is easily viewed in the SEM. The cavity and plate are made of niobium, which has a superconducting transition temperature of $T_c = 9.26$K. We operate the cavity in the TM_{020} mode at a resonance near 5.8 GHz. The cavity cross section is shown in Figure 2. The dark region is the removable plate. At the center of the plate is a "dimple" 3 mm in height and 12 mm in diameter. The dimple shape enhances the electric field at the dimple surface. Figure 2 also shows the radial profile and electric field distribution at the dimple.

Our input power coupler is located at the top flange in Figure 2 and our transmitted power probe is at the flange on the left. We have the capability of measuring the forward power (P_f), reflected power (P_r), and transmitted power (P_t) from the cavity and viewing them on an oscilloscope. Our power source is an oscillator which allows us to adjust the frequency. This power is amplified with a 20 W or 200 W amp. A lock is attained at the resonance frequency through transmitted power feedback. The P_r scope trace shows the behavior of the cavity, allowing us to determine when we are in lock and when we are unity coupled. An x-ray detector and a current probe provide information about field emission during a test. The P_t probe dually serves as the current probe. So far we have not seen any activity from the current probe though we have had much electron field emission.

Details regarding cavity measurements during testing are described in sec-

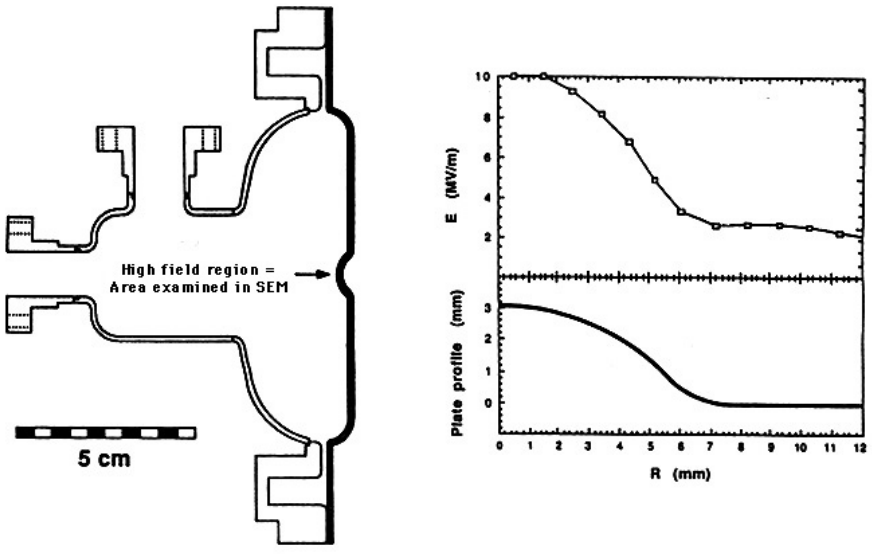

Figure 2: The diagram on the left shows a cross section of the mushroom cavity. The removable end plate has a dimple where the electric field is a maximum. The plot on the right shows the electric field distribution and the plate profile near the dimple for the TM_{020} mode.

tion 4.4. A thorough overview of the microwave components and a schematic of the setup can be found in reference [3].

4 Procedure

There are numerous steps involved in our procedure. In summary they are: preparing the plate, scanning the dimple, mounting the plate, RF testing, and post-test examination in the SEM. Each step is described in greater detail below.

4.1 Preparing the Plate

Once a type of particle and a plate are chosen, we prepare the plate as follows: The niobium mushroom plate is placed in nitric acid for 1 hour to remove residual indium left from the vacuum seal. It is then chemically etched in Buffered Chemical Polish (BCP) which consists of nitric acid, hydrofluoric acid, and phosphoric acid in a 1:1:2 ratio respectively. We etch for 10-15 minutes at temperatures between 12-15 °C. The etch rate is approximately 1-2 μm per minute. The plate is then rinsed in ultra-pure deionized water for 45 minutes and allowed to dry in a class 100 clean room. Once dry, the indium seal is formed and pressed at 2000 psi onto the edge of the plate.

A solution of the particle powder in methanol is prepared. The desired concentration of powder is determined through calculations and/or previous testing of various concentrations. Powders we used were nickel, molybdenum disulfide, and glassy carbon splinters (see Figure 3). The solution is taken into a class 1000 clean room, the rest of the methanol is added, and it is placed in an ultrasonic cleaner for 10 minutes to break up large clumps of particles. In a class 100 clean room the solution is stirred and a portion selected with a syringe is filtered to remove particles >5 μm in size. A glass capillary tube, 0.4 mm inner diameter, is used to deposit a drop on the dimple. A drop is always placed at the center of the dimple and at times also on the side to have particles at different field levels. The drop is usually 5-10 mm in diameter. If the drop is unsatisfactory we thoroughly wipe the dimple with methanol and a clean wipe before trying again. The drop is allowed to dry for several minutes before placing in the SEM chamber.

4.2 Scanning the drop

The plate is placed in the chamber of the SEM and the coordinates of the dimple center are estimated to within approximately $\pm$ 0.5 mm. The boundary of a methanol drop is visible due to crystallized methanol at the edge. The drop is systematically scanned at 300-400X magnification and foreign particles are photographed at this magnification (to aid in later locating) and at close range. The position is noted in terms of the SEM x and y-coordinates, and the elemental composition of the particle is determined through EDX analysis. This

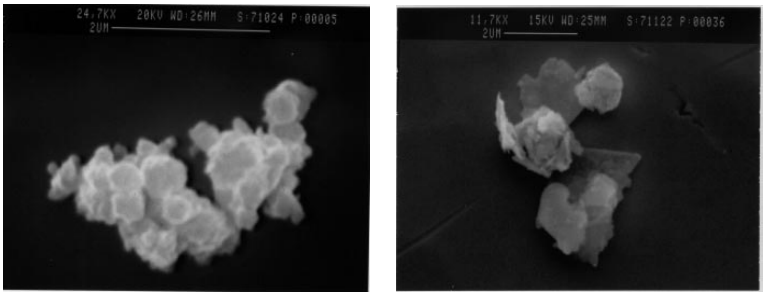

(a) (b)

Figure 3: Particles we deposited on mushroom plates: (a) Nickel, (b) Molybdenum disulfide (MoS_2).

is a time consuming process and thus it is desirable to take care in preparing a good plate so that scanning is not done in vain.

4.3 Mounting the plate

When the scanning is complete, the cavity test stand is wiped down and brought into the class 100 clean room. The cavity is bled up to atmosphere with nitrogen gas and is left slightly over-pressured at 1/2 psi. The clamps are removed and a large pipe cutter is used to break the indium seal between the cavity and plate. One person supports the cavity to keep it from deflecting while the other uses the pipe cutter. This is a delicate procedure and the Nb joint has deformed over the years. (When removing the plate to get ready for our last test of the semester that joint cracked). Once the plate is removed and the residual indium is scraped from the cavity, the new plate is taken out of the SEM and the old plate is placed in it. The new plate is aligned, the N_2 gas turned off, and the plate is clamped down by systematically tightening the bolts. The cavity is pumped down to roughly 10^{-7} torr with a turbo pump and then is placed on an ion pump.

4.4 Testing the cavity

The test stand is placed in a dewar. The outer jacket is filled with liquid N_2 and then approximately 90 L of liquid He is transferred. During the transfer (while the cavity is at 4.2 K) we find the resonant frequency of the cavity. Typical values are near 5.8 GHz. Once the transfer is complete and the resonance determined, we pump down the vapor space of the He to ~ 6 torr which brings the temperature of the cavity to about 1.4 K. The cavity resonant frequency usually decreases by several MHz during the pump down.

Once locked on resonance at 1.4 K we begin at low power ($P_i \sim 0.1$ W) and adjust the coupler to obtain unity coupling ($\beta = 1$). We use the P_r signal in modulated mode for feedback about the coupling and general behavior of the cavity. We measure the decay time τ_L of the emptying peak to obtain the relation (when $\beta = 1$) between stored energy U and the incident power P_i:

$$U = 2P_i\tau_L$$

We also measure the continuous wave (CW) value of P_t to obtain the constant in the relation:

$$U = c_t P_t$$

Once these relationships are determined we make measurements at successively higher input power (in steps of 2 dB). At $\beta = 1$ we record the CW values of P_t and P_f which give us E_{peak} and Q by the following relations:

$$E_{peak} = 215\sqrt{U}$$

$$Q = \frac{(1+\beta)^2}{4\beta}\frac{\omega U}{P_i}$$

From the data we plot Q vs. E_{peak} curves, an example of which is shown in Figure 4. As higher fields are reached we begin to detect x-rays from the cavity using a Geiger counter. As the fields increase, the intensity of the x-rays generally increases as well. Finally in all of our successful tests we reached a field at which thermal breakdown occurred. Either a defect in the cavity or the field emitting electrons impacting the surface caused the cavity to go normal conducting. The highest fields we have reached on successful tests ranged from 44 MV/m to 75 MV/m.

4.5 Post-test examination in the SEM

After the plate is removed we examine it again in the SEM. We locate all the sites that were photographed initially and note and photograph any changes. We also examine all starbursts on the dimple, whether correlated to a known particle or not.

5 Description of Tests

During the semester we attempted 8 tests (see Table 1 for a brief listing). The first two were practice runs to become familiar with the equipment. Three of the later tests were successful. The practice runs were done with the plate IA2 already on the cavity from its years of storage. We reached E_{peak} values of 54.2 and 60.9 MV/m respectively during these tests.

For our first particle placement test we attempted to put nickel particles on the dimple of plate IA1. No nickel particles were found during scanning, however enough other debris was on the dimple that we decided to test the

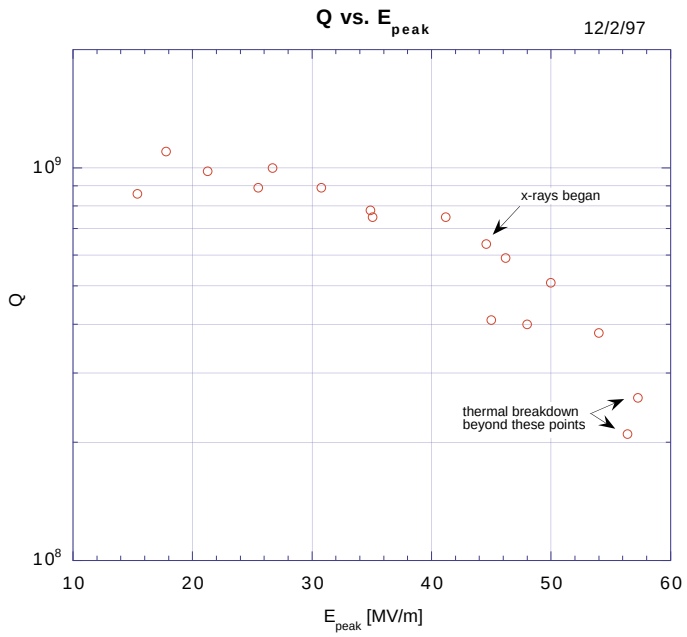

Figure 4: The Q versus E_{peak} plot for our 12/2/97 test of plate IA2. This plate contained a MoS_2 particle and silicon and carbon particles.

Table 1: A list of mushroom cavity tests preformed during Fall 1997.

Date	Plate	Placed Particles	E_{peak}	Changed Particles	No. of Starbursts
8/15/97	IA2	(test run)	54.2 MV/m		
8/19/97	IA2	(test run)	60.9		
9/12/97	IA1	none	75.3	Si, C	30
9/24/97	C5	Ni	43.9	Si	1
10/20/97	C6	Ni	(test unsuccessful)		
11/8/97	IA2	(test run)	(locking circuit difficulties)		
12/2/97	IA1	MoS_2	58.1	Si+O	10
Dec. '97	IA2	MoS_2, C	(cavity cracked)		

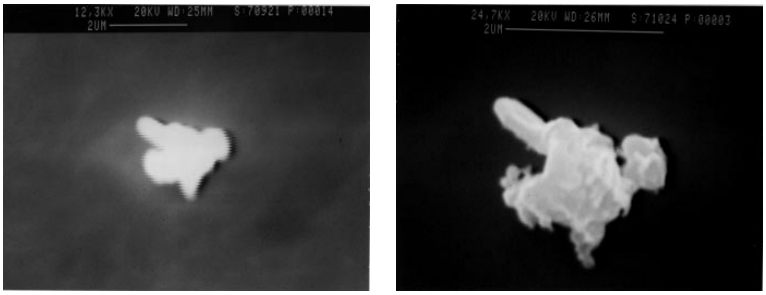

(a) (b)

Figure 5: A nickel particle (a) before and (b) after testing. $E_{peak} \sim 43.9$ MV/m in this region. No change is apparent, though comparison is limited by the poor quality of the before picture (a).

plate anyway. There were several silicon particles and carbon particles, as well as a magnesium-calcium particle. At the center of the dimple there was a large (~ 25 μm) scratch in the Nb that gave some EDX signals of silicon. We believe this scratch came from the capillary tube used to deposit the drop. During the test we reached $E_{peak} = 75.3$ MV/m. At 47.3 MV/m x-ray signals began and they increased greatly in intesity as the field increased. Approximately 30 starbursts were found on the dimple after the test. Of the particles, one of the larger silicon particles exploded and a carbon particle changed its appearance. These findings will be discussed in section 6. We were unable to locate some of the smaller particles seen before testing after the test, but there were no starbursts where these particles should have been.

We successfully deposited about a dozen nickel particles on plate C5 for our next test. The nickel ranged in size from 2 to 4 μm. There were also several silicon particles observed during scanning. This plate only reached $E_{peak} = 43.9$ MV/m before encountering thermal breakdown. Some x-rays were detected above $E_{peak} \sim 40$ MV/m and one starburst was seen afterwards in the SEM. None of the nickel particles appeared to change significantly (see Figure 5 for one example) and none were located in the starburst. Detailed before and after comparison of the nickel surface was not possible because of the poor quality beforehand pictures. One of the silicon particles melted.

For our third plate we deposited nickel on C6. We hoped to bring this plate to higher fields and obtain better before pictures. During the test we were unable to get transmitted power and had to abandon the test. We replaced the transmitted power cable, though the network analyser showed nothing wrong with it. We found no large debris on the inside of the cavity when the plate was removed. We mounted a freshly etched plate (IA2) and tested the cavity again. We were able to get transmitted power, though we had some trouble

with the feedback. After the test we realized we were probably giving it to much feedback. Having obtained a measurable P_t we proceeded on with the project.

We attempted to deposit nickel and molybdenum disulfide particles on plate IA1. Since our previous test with nickel showed no interesting results we decided to try it again, and the molybdenum particles were known to have jagged edges, thus making them likely field emitters. No nickel was found, but there was one MoS_2 particle, and carbon, indium, iron, and silicon-oxygen (with lesser amounts of sodium and aluminum) particles. This test ran successfully. We achieved an E_{peak}=58.1 MV/m and detected x-rays beginning at 44.6 MV/m, increasing in intensity as the field increased. Approximately 10 starbursts were found. The only particle change occurred with the Si+O particles. Two of them melted. One of the indium particles seemed to change by a small amount, but the original picture is not sharp enough to tell.

We planned to do one more test and had deposited MoS_2 and glassy carbon splinter particles on plate IA2. However, we discovered a large leak in the cavity vacuum when we tried to pump down after mounting this plate. Apparently the niobium joint connecting the upper flange to the cavity cracked while removing the previous plate. This happened several years ago as well to this cavity's predecessor. We are hopefully going to have the old cavity welded and continue testing placed emitters next semester.

6 Results

We did not see as much field emission from our placed particles as we hoped for. None of the purposely placed particles (Ni, MoS_2) changed at all during testing. However, it must be noted that we were only able to test three plates successfully, and the concentration of placed potential emitters was low on two of the plates. We did see several interesting effects with incidental particles of silicon and carbon. It was always the larger particles that changed. Details and discussion of these results follow.

6.1 Explosion of a Silicon Particle

Our most exciting result came from a 15 μm silicon particle. This particle had sharp edges and many jagged protrusions. It exploded and left behind a cluster of starbursts, melted Nb, and an elaborate pattern of residue. See Figure 6 for the close up before and after pictures and Figure 7 for the surrounding starburst pattern. EDX analysis applied to multiple spots of the residue showed no silicon signal. However, there is probably a thin layer of silicon undetectable by this method. Previous experiments support this, as only 50% of central craters in starbursts showed EDX signals of a foreign particle, yet in subsequent Auger Electron Spectroscopy a foreign particle layer was always detected [4]. The white hazy layer around the residue could be silicon.

(a)

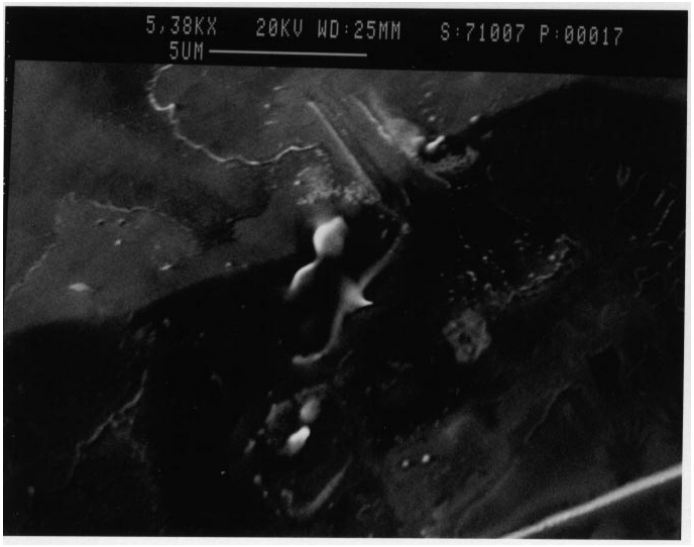

(b)

Figure 6: (a) The silicon particle before the RF test. (b) The residue of the silicon particle after the explosion. See Figure 7 for a zoomed out view of (b).

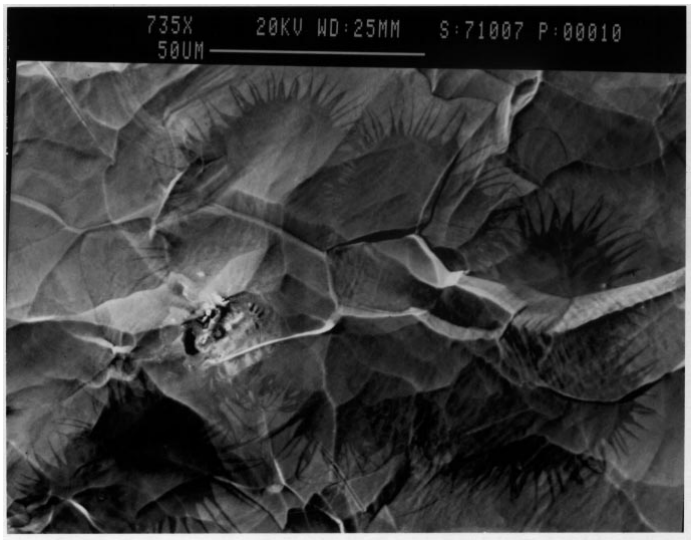

Figure 7: The starburst pattern surrounding the exploded silicon particle.

It is not surprising that this particle field emitted and then processed. The many jagged edges could have provided great geometrical field enhancement. The highest (non-enhanced) field attained at the site was more than enough, given past data, to allow field emission and processing. The peak field for the cavity was 75.3 MV/m. This site was 2.2 mm from estimated center and thus fields there were at least 90% that of the center. The activity at this site probably started at a field below this maximum level, and it could have begun at a field as low as 90% of 47.3 MV/m (the field at which the first x-rays were detected during the test).

The starburst pattern at the site is interesting. There is not a large starburst centered about the particle's location. Rather, there seems to be a cluster of at least six 50 μm starbursts to the right of the residue and two to the lower left. Perhaps there was not a uniform plasma surrounding the entire particle. It seems that there are more jagged edges on the particle on the lower long side and at the tips (short sides). This roughly corresponds to the location of the starbursts. Perhaps those were the field emitting protrusions and the plasma density was greatest around them. Since the particle is larger than most previously observed emitters it may be feasible for the plasma gas density to vary over the particle. When the particle exploded the areas of greatest plasma density created starbursts. Some of the rightmost starbursts could be secondary starbursts, caused by field emission of the niobuim surface excited by the nearby activity.

Another point to note is that there are no craters where the particle was, though there is some melted niobium. There are two small craters in the lower left starburst. No foreign elements were detected with the EDX at these craters.

These craters could be secondary ones from field emitting niobium, or there could have been a small undetected foreign particle there for which field emission was triggered by the nearby activity or that separately processed. One could argue that a piece of silicon shrapnel from the large particle's explosion landed there (30 μm away) and separately processed. However that is a large distance to travel. None of the starbursts in the cluster to the right had visible craters or foreign particles. The absense of a crater at the particle site suggests that the explosion differed a bit from those of other processed sites described in reference [5]. This is consistent with the absence of one large surrounding starburst.

There is no conclusive theory to indicate why the starbursts have the arrangment they do and why the residue looks as it does. Future examination of similar particles and processing would further the understanding. The complexity of the residue and the starburst pattern do not suggest a simple theory describing the events.

6.2 Melting of Silicon Particles

In addition to the complex explosion described in the last section, several silicon particles changed in another way: they melted. In three cases the melted region encompassed most of the particle, indicating RF heating instead of heating due to field emission current.

One 15 μm silicon particle melted during the second test (see Figure 8). The entire particle melted and thus it was probably a result of RF heating. This particle was exposed to a maximum field of $\sim$ 44 MV/m (at a distance 1 mm from the dimple center). The limited number of detected x-rays also does not suggest field emission. RF heating may have been enhanced if the particle was only weakly connected to the surface. The dark horizontal shadows in the after picture indicate that the particle was charging from the electron beam. This would happen if particle was mostly isolated from the niobuim. The before picture does not exhibit this behavior though so it was probably sufficiently attached to the surface initially. Previous research has shown that melting can weaken interface with the surface due to "necking" [1].

Two silicon based particles (8 μm and 6 μm across) mostly melted during our last test (see Figure 9). EDX analysis showed the particles to be mostly Si and O, with some Al and Na. These particles were 0.15 mm from each other and reached a maximum field of 58.1 MV/m. Again, RF heating is the likely phenomenon behind the melting. For both particles there is an unmelted region to the left of the melted sphere. This suggests that the unmelted region was better connected to the niobium surface. Another hypothesis is that since the particles were in close proximity to each other and both had regions on the left that did not melt, perhaps the RF heating was stronger to the right.

Note that the size of the particles decreased during melting. This of course is logical because a spherical shape gives the smallest dimensions for any given volume. The three melted silicon particles went from 15 to 9 μm, 8 to 3 μm, and 6 to 5 μm respectively.

There was one other silicon particle (5 μm) that showed evidence of melting

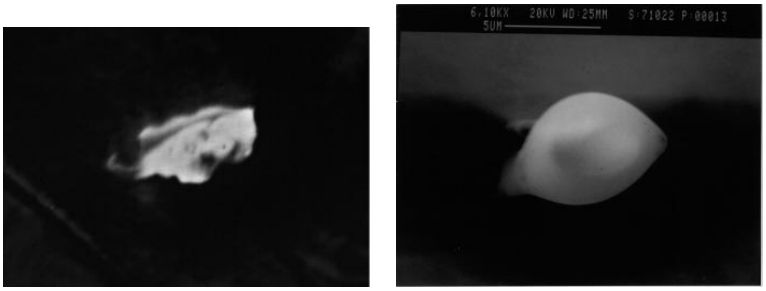

(a) (b)

Figure 8: A 15 μm silicon particle (a) before and (b) after RF testing. The melting is most likely due to RF heating.

around the edges. This particle reached a maximum field of 75.3 MV/m which is higher than that of the 3 which melted almost completely. There were also other silicon particles (less than 5 μm in size) in comparable electric fields that did not melt at all. Two hypotheses are that larger particles are more susceptible to RF heating and/or that the melted particles were less attached to the surface and thus could not conduct the heat away.

6.3 Breaking and Spot Melting of a Carbon Particle

The final interesting result was the change in the 32 μm carbon particle in Figure 10. It appears as 3 segments in the after photo and the 10 μm section in the lower right of the before picture is gone leaving only a faint outline. There is also a small molten sphere (less than 1 μm) on the lower edge of the largest segment. A bright speck can be seen in the before photo where the melted region is in the after shot. This fleck is probably carbon as well, though it could be another substance. Field emission is the likely cause of this melted spot. At high enough fields the fleck probably began emitting electrons and the current rose enough to melt the region. However there was not enough activity to create a starburst. An alternate explanation is that the fleck was not firmly attached to the base particle and it melted due to RF heating.

Another question to address is why the particle became 3 pieces. The missing segment from the lower right could have been ripped away by RF forces. The remaining 3 segments look as if the carbon between them vaporized. There is a hazy ring surrounding these gaps suggesting vaporization or a similar process. The question is how could vaporization occur and why are the other segments intact. Perhaps other points on the particle began to field emit or were subject to RF heating. The FN current could have risen enough to vaporize the underlying carbon. Perhaps the structure of the C particle was such that the missing and untouched regions were isolated from each other and/or differed in their interface

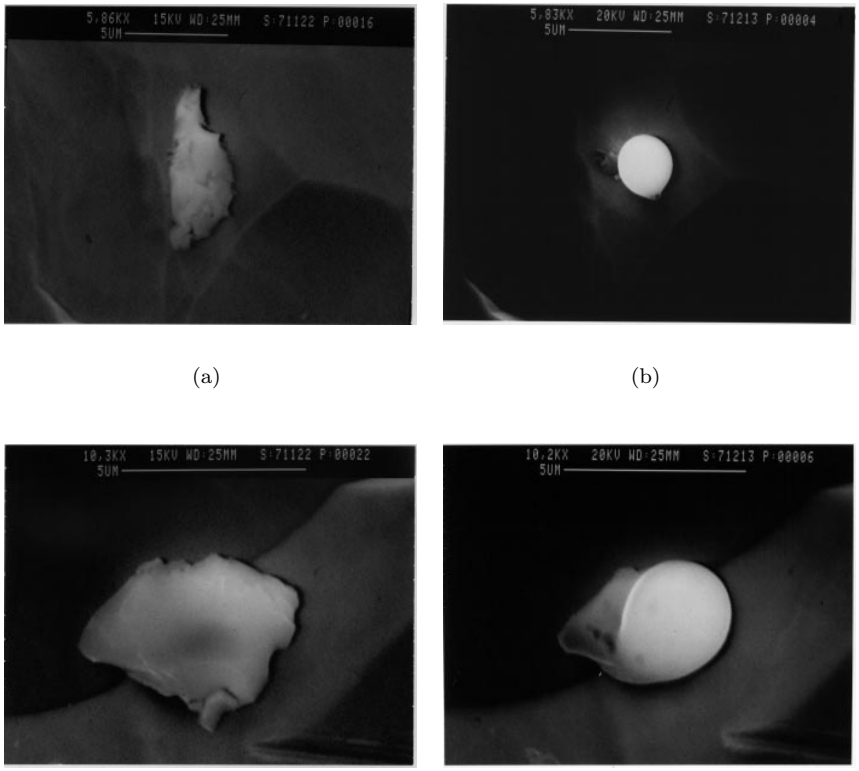

(a) (b)

(c) (d)

Figure 9: An 8 μm silicon particle before (a) and after (b) RF testing. A 6 μm silicon particle prior to (c) and after (d) RF testing. The particles were on the same mushroom plate and were 0.15 mm from each other. The melting is most likely due to RF heating.

(a)

(b)

Figure 10: (a) A 32 μm carbon particle before RF testing. (b) The carbon particle after testing. Note the small melted spot and the missing segments.

with the surface.

The melting and boiling points for carbon and silicon at standard pressure are

element	melting pt	boiling pt	sublimation
carbon	3550 °C	NA	3367 ±25 °C (graphite)
silicon	1410 °C	2355 °C	

These temperatures are obviously not accurate for cavity vacuum pressure of $< 10^{-8}$torr. These phase changes will occur at lower temperatures for lower pressure. However, it is reasonable to assume that temperatures for carbon remain higher than those of silicon, and that sublimation of graphite from solid to gas would still occur. Carbon melts at higher temperatures than silicon, so it is more likely to find melted silicon than melted C on the plate. Note also that the sublimation temperature for graphite is lower than its melting point. If the C particle in Figure 10 is graphite, which is reasonable given its appearance, then it should sublime before it would melt. Thus the vaporization hypothesis for the missing segments is possible. This reasoning suggests that the melted speck either is not carbon or is carbon in a different form since it did melt.

7 Discussion

The results of this project begin to show some correlations between the initial properties of a particle and the outcome at high electric fields. We have seen that silicon is altered most frequently. The most jagged silicon particle exploded while others just melted. In all cases where change occured, the particle was larger than 5 μm. Perhaps because larger particles protrude more they provide greater field enhancement and are more susceptible to RF heating. The nickel and MoS_2 particles did not do anything, but field emission is certainly not ruled out for these particles. The nickel was only brought to 44 MV/m which perhaps was not great enough to excite them. Futhermore, studies have shown that only 5-10% of particles field emit [1], so perhaps the nickel could have emitted but just didn't. We only had one MoS_2 particle, so though it was jagged, probability predicts that it would not emit.

We hope to continue this research during the spring semester. There are several approaches we may take to acquire more data. First, we will be more aggressive with our particle placement. The number of particles we placed did not seem to have an adverse effect on Q_o vs. E_{peak} during testing, so we will increase our numbers and see what happens. More particles theoretically means more field emitters. We may also try new particles such as gold or copper as well as additional tests with MoS_2 and perhaps carbon and nickel. We may attempt to understand silicon better by intentionally placing it there, though it is naturally occuring too.

To understand the E-field dependence of the triggering of field emission we will put at least 2 drops of the solution on the dimple: one in the center and one on the side (where fields are lower). The distance of the particle from the dimple center will determine the peak field reached. If field emitters turn on

only within a certain radius from the center that will give us a lower bound for field emission of that type of particle. We have placed multiple drops on the dimple occasionally during previous tests, but results have been inconclusive thus far.

Another aspect we may want to explore is the dependence of field emission on the interface between the particle and the niobium. Through heat treatment it has been shown that the number of field emitters depends upon the interface. Currently we don't have a method of exploring this with the mushroom plate. A possible method could involve current measurement with the SEM. The electron beam creates a current in the plate which is detected and displayed. When the beam is focused on a particle, the current probably depends on the ability of the particle to conduct to the surface niobium. The better the interface, the more current would be transmitted. If we were to record the current measurements before a test and quantify them, perhaps that could give us information about the interface. This would increase scanning time, but it might be something to explore once we have more data.

8 Summary

The goal of this study is to increase our understanding of field emission by correlating images of emitters before and after RF testing. We used the "mushroom" cavity for these experiments and deposited various particles on the high field dimple. We saw no field emission signatures from nickel, though our data was limited. Our results include several particle changes: an exploded silicon particle, a partially vaporized carbon particle, and several melted silicon particles due to RF heating. These results have suggested a few issues for further explanation such as why do some particles melt and not others, how does the particle interface with the surface affect emission and RF heating, and does the plasma density during emission vary over the surface of a particle. We plan to refine our procedure and continue these tests, hopefully acquiring more results from particles intentionally placed on the surface. Future results may provide some answers to our questions and raise more questions regarding the theories of field emission.

References

[1] H. Padamsee, J. Knobloch, T. Hays. *'RF Superconductivity for Accelerators'*. (1998), Ch. 12. (To be published). (To be published), Ch. 12.

[2] J. Knobloch and H. Padamsee, *Particle Accelerators*, **53** (1996), 53.

[3] K. Green. *'An Introduction to Coaxial Microwave Systems'*. Cornell Univ. Laboratory of Nuclear Studies. (1989).

[4] T. Hays, et al., *Proceedings of the 6th Workshop on RF Superconductivity*, edited by R. M. Sundelin, CEBAF, Newport News, Va., (1994), 750.

[5] D. Moffat, et al., *Particle Accelerators*, **40** (1992), 85.